ISSN 1063-7761, Journal of Experimental and Theoretical Physics, 2011, Vol. 112, No. 1, pp. 108–120. © Pleiades Publishing, Inc., 2011.
Original Russian Text © V.V. Val'kov, M.M. Korovushkin, 2011, published in Zhurnal Eksperimental'noi i Teoreticheskoi Fiziki, 2011, Vol. 139, No. 1, pp. 126–139.

ORDER, DISORDER, AND PHASE TRANSITION IN CONDENSED SYSTEM

Splitting of the Lower Subband of Hubbard Fermions in the Shubin–Vonsowsky Model under the Influence of Strong Intersite Correlations

V. V. Val'kov[a,b,*] and M. M. Korovushkin[a]

[a] *Kirensky Institute of Physics, Russian Academy of Sciences, Siberian Branch, Krasnoyarsk, 660036 Russia*
[b] *Reshetnev Siberian State Aerospace University, Krasnoyarsk, 660014 Russia*
**e-mail: vvv@iph.krasn.ru*

Received May 7, 2010

Abstract—The diagram technique for Hubbard operators is used to investigate the influence of intersite Coulomb interactions on the energy structure and Cooper instability of strongly correlated fermions. Allowance for intersite correlations in doped Mott–Hubbard insulators is shown to lead to a splitting of the lower subband of Hubbard fermions and to the formation of a band of fluctuation states as soon as the intersite interaction energy becomes comparable to or exceeds the mean kinetic energy. The spectral intensity of the split-off band is proportional to the root-mean-square fluctuation of the occupation numbers and increases with doping level. The predicted effect changes significantly the structure of the density of electronic states. This leads to a renormalization of the pole of the scattering amplitude in the Cooper channel and manifests itself as a nonuniform (in electron concentration) modification of the dependence of the critical superconducting transition temperature.

DOI: 10.1134/S1063776110061056

1. INTRODUCTION

One of the remarkable examples of a nontrivial manifestation of many-body effects in condensed matter physics is the metal–insulator transition [1]. This transition can take place in a system of collective electrons in the case of electron concentration $n = 1$ per unit cell as the energy of the Coulomb interaction between electrons increases to values comparable to or exceeding the mean kinetic energy. The Hubbard model [2] is used most commonly when this approach is studied theoretically. In this model, the Coulomb interaction only between the electrons on one ion and with opposite spin moment projections is taken into account. The approach based on the atomic representation [3] and the diagram technique developed for Hubbard operators (DTH) in [4] proved to be efficient in describing such systems. The authors of [5–7] pointed out restrictions related to the use of the Hubbard model in describing the Mott transition in real materials and developed a theory of this transition based on the more realistic Shubin–Vonsowsky model [8, 9]. In this model, apart from the Coulomb repulsion of electrons on one site, the intersite Coulomb interaction, which may turn out to be significant near the dielectric phase due to the degradation of screening, is also taken into account. Using the diagram form of the perturbation theory allowed one to calculate the correlation effects related to the inclusion of intersite interactions and to study the influence of these effects on the Cooper instability in the Shubin–Vonsowsky model [10]. The nontrivial role of the Coulomb interaction in the occurence of Cooper pairing with a nonzero total momentum was discussed in [11]. The influence of intersite interactions on the energy structure, the formation mechanism of the pseudogap behavior, and the superconducting pairing of strongly correlated electrons were studied in [12, 13].

Here, we consider the effect that should be expected for narrow-band compounds when the hopping integral comparable to the intersite Coulomb repulsion parameter. The dependence of the one-site electron energy on the configuration environment will manifest itself in this case. To elucidate the effect, let us consider the limiting case where the hopping integral becomes zero. In this case, all one-electron energies can be found exactly. In particular, for a simple cubic lattice where there is one electron on each of z nearest neighbors, the "setting" energy of the electron on the central ion will be determined not just by the seed one-site energy ε_0 but by the renormalized expression $\varepsilon_0 + zV$, where V is the parameter that defines the Coulomb interaction of two electrons on neighboring sites in the Wannier representation. If one electron is absent on the ions in the immediate neighborhood of the site under consideration, then the setting energy will be different: $\varepsilon_0 + (z-1)V$. This simple reasoning shows that when the configuration environment deviates from the nominal one, one should expect the appearance of states with energies differing by V in the spectrum of Fermi excitations.

If the relatively weak hopping integral is included, when a narrow band of Fermi states is formed, the described effect will lead to a splitting of the original band of Fermi states. Note that this splitting is not related to the well-known Hubbard two-subband formation mechanism and will manifest itself as an additional splitting of the lower (or upper) Hubbard subband. Obviously, the higher the probability with which the electronic configuration of the environment will deviate from the nominal one, the higher will be the spectral intensity of the split-off band. The root-mean-square (rms) fluctuation of the occupation numbers will act as a quantitative measure of this deviation. Bearing this in mind, below we will call the split-off band a band of fluctuation states (BFS). For undoped Mott–Hubbard insulators, the electronic configuration of the environment corresponds to the nominal one. In the case of doping, the nominality will break down and BFS whose spectral intensity will increase with doping level will appear in the spectrum.

The presentation of our results is organized as follows. In Section 2, we formulate the main physical assumptions under which the manifestation of intersite Coulomb interactions in the properties of strongly correlated systems will be analyzed. Based on the atomic representation in the Shubin–Vonsowsky model, we demonstrate the physical mechanism that leads to the dependence of the electron setting energy on the ion configuration environment and to the induction of BFS. In Section 3, we introduce a smallness parameter that allows the main diagrams for the mass and strength operators to be selected. Based on this approach, we calculate the one-site propagator that acquires a two-pole structure due to the renormalization of the electron setting energy noted above. The formation of a split structure of the lower Hubbard subband induced by relatively strong intersite Coulomb correlations is discussed in Section 4. Here, we also present data on the redistribution of the total spectral intensity based on numerical calculations. The predicted effect is shown to be stable against allowance for the scattering processes in Section 5. The results of our calculation of the scattering amplitude in the Cooper channel obtained by taking into account the contributions from BFS are presented in Section 6. We demonstrate a nonuniform (in electron concentration) renormalization of the critical superconducting transition temperature. The results obtained are discussed in the final section.

2. THE HAMILTONIAN OF THE SYSTEM IN THE ATOMIC REPRESENTATION

To demonstrate the effect in the simplest form, let us consider the Shubin–Vonsowsky model in the regime of strong one-site electron correlations ($U \longrightarrow \infty$) at electron concentrations $n \leq 1$. In this case, the electronic properties of the system in the atomic representation will be determined by the lower Hubbard subband. Taking into account the arguments of [5, 7], we will restrict our analysis to the Coulomb interaction only between the electrons on neighboring sites. The system of Hubbard fermions will be described by the Hamiltonian

$$\hat{H} = \sum_{f\sigma}(\varepsilon_0 - \mu)X_f^{\sigma\sigma} + \sum_{fm\sigma} t_{fm} X_f^{\sigma 0} X_m^{0\sigma} + \frac{V}{2}\sum_{f\delta} \hat{n}_f \hat{n}_{f+\delta}. \quad (1)$$

Here, the first term reflects the ensemble of noninteracting Hubbard fermions in the Wannier representation. The appearance of a fermion with spin projection $\sigma = \pm 1/2$ on site f increases the system's energy by ε_0, μ is the system's chemical potential, $X_f^{pq} = |f, p\rangle\langle f, q|$ are the Hubbard operators [3] that describe the transition from a one-site state $|q\rangle$ to a state $|p\rangle$. The second term corresponds to the kinetic energy of the Hubbard fermions, where the matrix element t_{fm} defines the intensity of the electron hopping from site f to site m. The last term in the Hamiltonian takes into account the Coulomb interaction of the electrons on neighboring sites f and $f + \delta$ whose intensity is defined by the quantity V. The Hubbard fermion number operator for site f is defined by the expression

$$\hat{n}_f = \sum_{\sigma} X_f^{\sigma\sigma}.$$

In what follows, we will restrict our analysis to the case where the number of holes

$$h = \frac{1}{N}\sum_f \langle X_f^{00}\rangle$$

in the system is small, i.e., the inequality

$$h = 1 - n \ll 1 \quad (2)$$

holds. In this case, it is appropriate to separate out the mean-field effects attributable to intersite interactions in explicit form. Using the condition for completeness of the diagonal X operators in reduced Hilbert space

$$X_f^{00} + X_f^{\uparrow\uparrow} + X_f^{\downarrow\downarrow} = 1,$$

we will represent Hamiltonian (1) as

$$\hat{H} = -E_0 + \sum_{f\sigma}(\varepsilon - 4Vh - \mu)X_f^{\sigma\sigma} + \sum_{fm\sigma} t_{fm} X_f^{\sigma 0} X_m^{0\sigma} + \frac{1}{2}\sum_{f\delta} V(X_f^{00} - h)(X_{f+\delta}^{00} - h), \quad (3)$$

where $E_0 = 2NV(1-h)^2$ in the mean-field approximation defines the Coulomb interaction energy for a system that contains h holes per site. At $h = 0$, E_0 reflects the Coulomb interaction energy for a system where exactly one electron is present on each site. The renor-

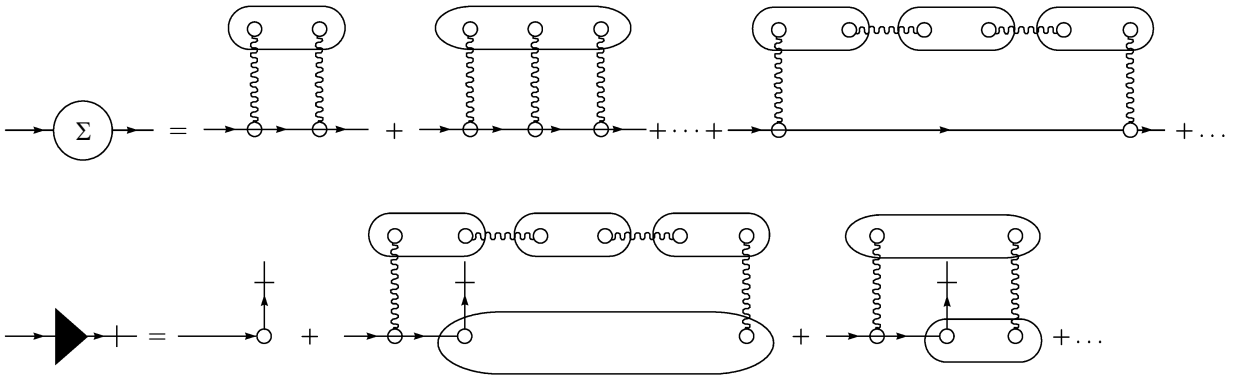

Fig. 1. Diagrams of the zeroth order in hopping parameter for the mass, Σ, and strength P, operators.

malized value of the one-electron level $\varepsilon = \varepsilon_0 + 4V$ is defined by the fact that the excitation energy increases by $4V$ if one electron resides on each of the neighboring sites. The shift of this level by $-4Vh$ is related to a decrease in the Coulomb repulsion energy if the mean number of holes in the system is nonzero.

Note that such mean-field renormalizations of the one-site electron energies were used previously, for example, in the Falicov–Kimball model [14] when transitions with a change in valence were investigated [15]. The meaning of the separation of obvious mean-field effects is to represent the intersite interaction in a form containing only the correlation effects. One can see that the last term in Hamiltonian (3) will make a contribution only in the presence of noticeable fluctuations in occupation numbers, i.e., at relatively strong intersite correlations.

3. THE SMALLNESS PARAMETER AND THE DIAGRAM SELECTION PRINCIPLE

To describe the energy structure of the system of strongly correlated fermions under consideration, let us introduce the Matsubara Green function [4]

$$D(f, \tau; f', \tau') = -\langle T_\tau \tilde{X}_f^{0\sigma}(\tau)\tilde{X}_{f'}^{\sigma 0}(\tau')\rangle$$
$$= \frac{T}{N}\sum_{\mathbf{k}\omega_n} \exp\{i\mathbf{k}(f-f') - i\omega_n(\tau-\tau')\} D(\mathbf{k}, i\omega_n) \quad (4)$$

and use the DTH. Consider a situation where the hopping parameter is small compared to the energy of the Coulomb repulsion of the electrons on neighboring lattice sites, i.e., $|t| \ll V$. In this case, allowance for the correlation effects attributable to the intersite Coulomb interaction acquires paramount importance.

One of the main DTH peculiarities is the existence of end diagrams [4, 16, 17]. Their complete set is called an end factor or a strength operator $P(\mathbf{k}, i\omega_n)$. The latter term was suggested in [18] when analyzing the diagram technique for spin operators. It follows from our analysis of the diagram series for the Fourier transform of the Green function that an exact representation relating $D_{0\sigma,\,0\sigma}(\mathbf{k},\, i\omega_n)$ to the mass and strength operators can be written as [16, 19]

$$D_{0\sigma,\,0\sigma}(\mathbf{k}, i\omega_n) = \frac{P_{0\sigma,\,0\sigma}(\mathbf{k}, i\omega_n)}{i\omega_n - \tilde{\varepsilon} + \mu - P_{0\sigma,\,0\sigma}(\mathbf{k}, i\omega_n)t_{\mathbf{k}} - \Sigma_{0\sigma,\,0\sigma}(\mathbf{k}, i\omega_n)}, \quad (5)$$

where $\Sigma_{0\sigma,\,0\sigma}(\mathbf{k},\, i\omega_n)$ is the mass operator and $\tilde{\varepsilon} = \varepsilon - 4Vh$.

For the Hubbard model in the limiting regime of strong correlations and an electron concentrations $n \le 1$, when passing to the atomic representation, only the hopping operator for the lower Hubbard subband acts as the interaction operator. In this case, the mass operator always contains the hopping parameter.

The situation in the Shubin–Vonsowsky model is different. Here, the perturbation operator is the sum of the kinetic energy operator and the operation describing the intersite interaction. Accordingly, the structure of the mass operator and the Green function becomes more complicated.

First of all, consider a modification of the one-site propagator attributable to intersite Coulomb correlations. The plots for the mass and strength operators in this case are formed from simple lines for one-site Green functions and wavy lines reflecting intersite interactions. Examples of such diagrams are shown in Fig. 1. On these diagrams, the ovals enclosing two, three, etc. small circles denote the cumulants of the second K_2, third K_3, etc. orders, respectively. The nth-order cumulant K_n is defined by the expression

$$K_n = \langle (X^{00} - h)^n \rangle. \quad (6)$$

Using the algebra of Hubbard operators allows an exact recurrence relation convenient for the calculation of cumulants K_n, $n \ge 2$, to be established:

$$K_n = (1-2h)K_{n-1} + h(1-h)K_{n-2},$$
$$K_0 = 1, \quad K_1 = 0. \quad (7)$$

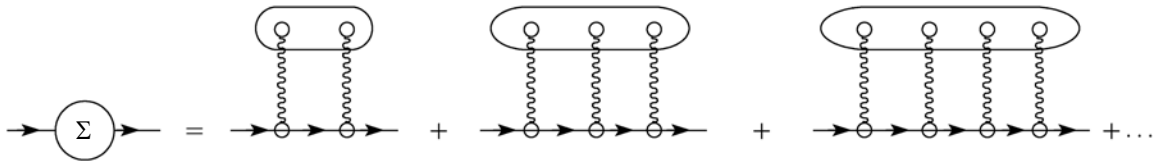

Fig. 2. Sequence of diagrams for the mass operator Σ.

It follows from these equalities that a parameter

$$\delta = h(1-h) \ll 1, \tag{8}$$

that is small at all values of h emerges in the problem of finding an analytical expression for the nth-order cumulant. For the subsequent analysis, it is important that an explicit dependence of the cumulant K_n on number n in the linear (in this smallness parameter) approximation is defined by the expression

$$K_n = h(1-h)(1-2h)^{n-2} + O(\delta^2), \quad n \geq 2. \tag{9}$$

We see that the cumulant of an arbitrary order has the first order of smallness in δ. Consequently, the plots containing one cumulant make a contribution of the first order of smallness in δ. The more cumulants enter into the diagram, the higher the order of smallness for this diagram. This reasoning shows that in the linear (in δ) approximation, it will suffice to restrict oneself to the contributions of those diagrams that contain only one cumulant. In our case, an infinite sequence of diagrams of the first order in δ for the mass operator has the form shown in Fig. 2.

Substituting the formula for the cumulant K_n, we see that the series for the mass operator

$$\Sigma_{\text{oval}}(i\omega_n) = \frac{zh(1-h)V^2}{i\omega_n - (\varepsilon - 4Vh)} - \frac{zh(1-h)V^3(1-2h)}{(i\omega_n - (\varepsilon - 4Vh))^2} + \frac{zh(1-h)V^4(1-2h)^2}{(i\omega_n - (\varepsilon - 4Vh))^3} - \ldots$$

is a geometric progression.

After the summation, we obtain a Matsubara-frequency-dependent mass operator for the one-site propagator:

$$\Sigma_{\text{oval}}(i\omega_n) = \frac{zh(1-h)V^2}{i\omega_n - (\varepsilon - V) + 2hV + \mu}. \tag{10}$$

It is easy to verify that the diagrams for the strength operator contain at least two cumulants. Therefore, in the linear (in δ) approximation, the strength operator is defined by the simple expression $P = 1 - n/2$. Taking these results into account, we find that the expression for the single-particle Green function acquires a two-pole structure:

$$D(\mathbf{k}, i\omega_n) = \left(1 - \frac{n}{2}\right)(i\omega_n - (\tilde{\varepsilon} - V(1-2h)) + \mu) \times ((i\omega_n - \varepsilon_{\mathbf{k}} + \mu)(i\omega_n - (\tilde{\varepsilon} - V(1-2h)) + \mu) - zh(1-h)V^2)^{-1}. \tag{11}$$

Here, $\varepsilon_{\mathbf{k}} = \tilde{\varepsilon} + (1 - n/2)t_{\mathbf{k}}$, $t_{\mathbf{k}}$ is the Fourier transform of the hopping integral.

It follows from Eq. (11) that the spectrum of Fermi excitations is defined by two branches,

$$E_{\mathbf{k}}^{\mp} = \frac{\varepsilon_{\mathbf{k}} + \zeta}{2} \mp \nu_{\mathbf{k}}, \quad \zeta = \tilde{\varepsilon} - V(1-2h), \quad \nu_{\mathbf{k}} = \sqrt{\left(\frac{\varepsilon_{\mathbf{k}} - \zeta}{2}\right)^2 + zh(1-h)V^2}. \tag{12}$$

We see that the resulting picture of the energy spectrum is formed through the hybridization of states from the ordinary Hubbard subband with energies $\varepsilon_{\mathbf{k}}$ and states induced by fluctuations of the configuration environment. The hybridization intensity is defined by a quantity proportional to the one-site rms fluctuation of the occupation numbers

$$\overline{(\Delta n)^2} = \langle (X_f^{00} - h)(X_f^{00} - h) \rangle = h(1-h).$$

After the analytic continuation, we find the spectral intensity

$$A(\mathbf{k}, \omega) = -\frac{1}{2}\operatorname{Im} D(\mathbf{k}, \omega + i\delta) = \left(1 - \frac{n}{2}\right)\left\{\left(\frac{1 + \lambda_{\mathbf{k}}}{2}\right)\delta(\omega - E_{\mathbf{k}}^{+} + \mu) + \left(\frac{1 - \lambda_{\mathbf{k}}}{2}\right)\delta(\omega - E_{\mathbf{k}}^{-} + \mu)\right\}, \tag{13}$$

where

$$\lambda_{\mathbf{k}} = \frac{\xi_{\mathbf{k}}}{\sqrt{\xi_{\mathbf{k}}^2 + zh(1-h)V^2}}, \quad \xi_{\mathbf{k}} = \frac{1}{2}\left(V(1-2h) + \left(1 - \frac{n}{2}\right)t_{\mathbf{k}}\right). \tag{14}$$

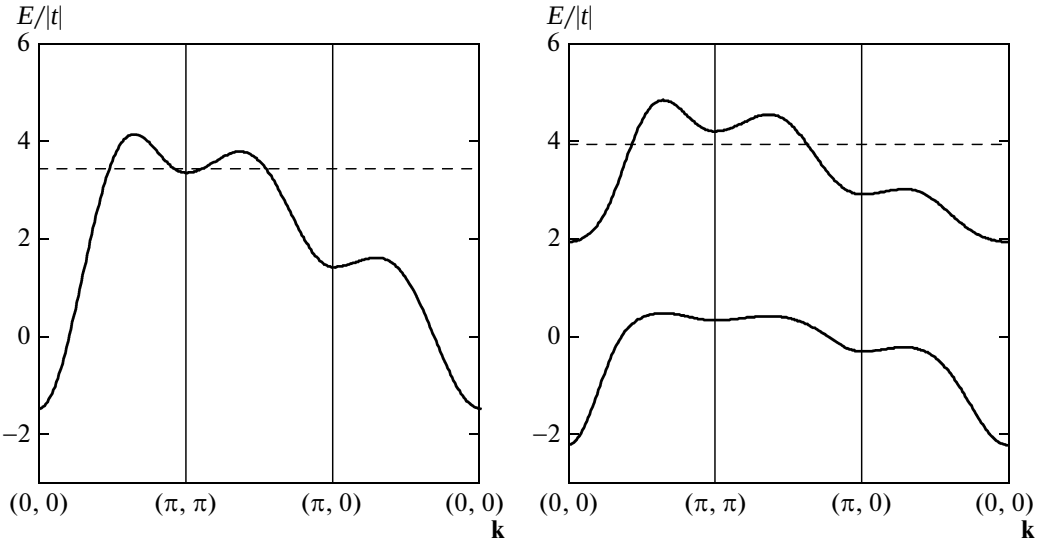

Fig. 3. Spectrum of Fermi excitations without (left) and with (right) allowance made for intersite correlations for the set of parameters $t' = -0.1$, $t'' = -0.5$, and $V = 2$ (in units of $|t|$) at hole concentration $h = 0.2$. The dashed lines indicate the position of the chemical potential.

It follows from Eq. (13) that the spectral intensity of the split-off band

$$A^{(-)}(\mathbf{k}, \omega) = \left(1 - \frac{n}{2}\right)\left(\frac{1 - \lambda_{\mathbf{k}}}{2}\right)\delta(\omega - E_{\mathbf{k}}^{-} + \mu)$$

in the regime $V \gg |t_{\mathbf{k}}|$ of interest to us is proportional to the rms fluctuation of the occupation numbers $\overline{(\Delta n)^2}$ introduced above:

$$A^{(-)}(\mathbf{k}, \omega) \approx \frac{4(1 + h)\overline{(\Delta n)^2}}{1 + 16\overline{(\Delta n)^2} + \sqrt{1 + 16\overline{(\Delta n)^2}}} \times \delta(\omega - E_{\mathbf{k}}^{-} + \mu). \quad (15)$$

Bearing this in mind, the split-off band may be considered as BFS. The spectral weight of BFS rapidly grows with increasing h. At the same time, the contribution of this band to the total density of states, which can reach 35% of the total density of states with increasing doping level, also grows (see Section 4).

When BFS is taken into account, the equation defining the relation between the chemical potential μ and the number of electrons n per site takes the form

$$\frac{n}{2} = \left(1 - \frac{n}{2}\right)\frac{1}{N}\sum_{\mathbf{k}}\left(\left(\frac{1 + \lambda_{\mathbf{k}}}{2}\right)n_{\mathrm{F}}(E_{\mathbf{k}}^{+}) + \left(\frac{1 - \lambda_{\mathbf{k}}}{2}\right)n_{\mathrm{F}}(E_{\mathbf{k}}^{-})\right), \quad (16)$$

where $n_{\mathrm{F}}(x) = (e^{(x-\mu)/T} + 1)^{-1}$ is the Fermi–Dirac function.

4. THE ENERGY STRUCTURE AT STRONG INTERSITE CORRELATIONS

Let us use the expressions derived above to calculate the energy structure of the system under consideration for a simple two-dimensional square lattice ($z = 4$). In this case, the Fourier transform of the hopping integral will be defined by the expression

$$t_{\mathbf{k}} = 2t(\cos k_x + \cos k_y) + R_{\mathbf{k}},$$
$$R_{\mathbf{k}} = 4t'\cos k_x \cos k_y + 2t''(\cos 2k_x + \cos 2k_y), \quad (17)$$

where t' and t'' are the hopping integrals into the second and third coordination spheres, respectively. Figure 3 (right) presents the band picture of the model under consideration calculated using Eqs. (12). This picture is compared with the calculation performed in the same model, at the same parameters, and for the same doping level but with allowance made for strong intersite correlations (SICs) in the Hubbard-I approximation (left). It follows from the comparison of the two presented spectra that a proper allowance for SICs leads to a qualitative difference that consists in the appearance of an additional band in the structure of the energy spectrum of the model.

In Fig. 3 (right), the upper energy band corresponds to the motion of an electron through the lattice sites at whose neighboring sites no holes are present. The characteristic setting energy of such an electron is $\varepsilon_0 + 4V$. The lower band describes the motion of an electron through the lattice sites at one of whose neighboring sites a hole appeared as a result of doping. The appearance of a hole in the immediate neighborhood reduces the setting energy of such an electron to a characteristic value of $\varepsilon_0 + 3V$. That is why the energy bands displayed in the figure are separated by the

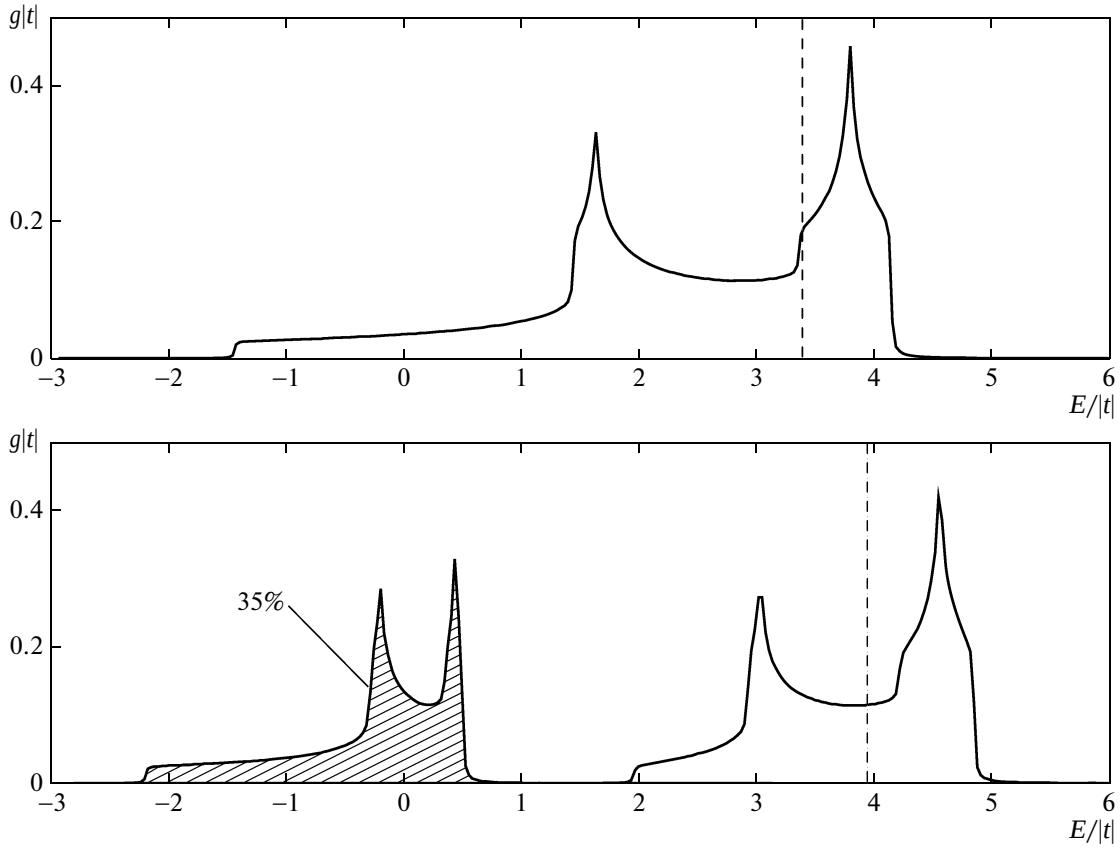

Fig. 4. Density of electronic states calculated without (top) and with (bottom) allowance made for intersite correlations for the set of parameters $t' = -0.1$, $t'' = -0.5$, and $V = 2$ (in units of $|t|$) at hole concentration $h = 0.2$. The dashed lines indicate the position of the chemical potential.

intersite Coulomb repulsion energy V. Obviously, allowance for the diagrams containing more than one oval would give rise to additional bands with characteristic energies $\varepsilon_0 + 2V$ and $\varepsilon_0 + V$. However, we do not consider this situation, because it corresponds to the case of high doping and violates conditions (2) and (8).

Thus, the formation of an additional band (BFS) is attributable to a change in the energy of the electron residing on a site if the electronic configurations deviate from the nominal ones near this site.

The appearance of BFS leads to a qualitative change in the form of the density of electronic states for Hubbard fermions. The upper plot in Fig. 4 shows the density of states for the model under consideration without allowance for intersite Coulomb correlations (ICCs). We see that ignoring these correlations leads to a trivial shift in the position of the band of Hubbard fermions. The lower plot in Fig. 4 shows the energy dependence of the total density of electronic states of the model for the same set of parameters but with allowance made for ICCs. Comparison with the upper plot shows that allowance for ICCs leads to a significant qualitative change in the form of the density of states: BFS is split-off and a gap is formed in the structure of the energy spectrum. For clarity, the density of BFS states $g^-(E)$ in this plot is represented by the line bounding the hatched region. In this case, BFS accounts for 35% of the total number of states of the system, while the main band with the density of states $g^+(E)$ accounts for 65% of the states. The addition of the densities $g^+(E)$ and $g^-(E)$ leads to the total density $g(E)$.

The plots presented in Fig. 4 were calculated at $h = 0.2$. If $h = 0$, then the contribution of SICs becomes zero and the density of states of the system will be as shown in the upper plot of Fig. 4. Hence follows the conclusion about the presence of a qualitatively new effect associated with allowance for SICs: doping leads not only to a shift in chemical potential but also to a rearrangement of the form of the density of states.

5. THE LADDER AND BORN APPROXIMATIONS FOR THE SCATTERING AMPLITUDE

When holes appear in the system, the energy structure will also be modified through the scattering processes attributable to the kinematic interaction between Hubbard quasiparticles [4]. In addition, the

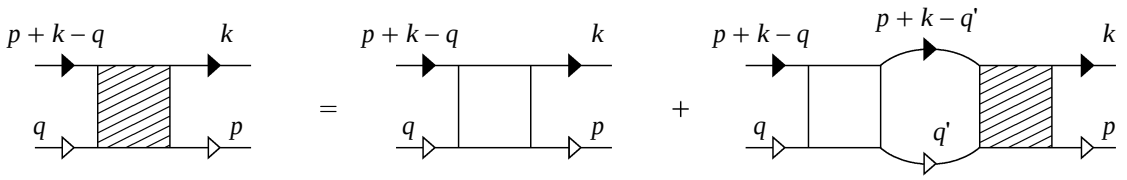

Fig. 5. Equation for the total scattering amplitude.

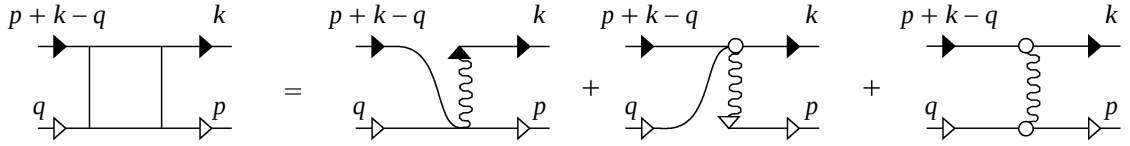

Fig. 6. Equation for the seed scattering amplitude.

contributions from the scattering by a Coulomb potential should be taken into account [7]. As a result, the scattering amplitude $\Gamma(q, p+k-q|p, k)$ in the ladder approximation obeys the graphical equation [4, 7, 16, 20] displayed in Fig. 5, where $p \equiv (\mathbf{p}, i\omega_n)$, $k \equiv (\mathbf{k}, i\omega_m)$, $q \equiv (\mathbf{q}, i\omega_l)$, $q' \equiv (\mathbf{q}', i\omega_{l'})$, while the seed amplitude (Fig. 6) does not depend on the Matsubara frequency and is defined by the expression

$$\Gamma_0(\mathbf{q}, \mathbf{p}+\mathbf{k}-\mathbf{q}|\mathbf{p}, \mathbf{k}) = V_{\mathbf{q}-\mathbf{p}} - t_{\mathbf{p}} - t_{\mathbf{k}}. \quad (18)$$

Accordingly, the amplitude $\Gamma(q, p+k-q|p, k)$ does not depend on the Matsubara frequency ω_l [20] and finding it is reduced to solving the integral equation

$$\Gamma(q, p+k-q|p, k) = V_{\mathbf{q}-\mathbf{p}} - t_{\mathbf{p}} - t_{\mathbf{k}} + \frac{1}{N}\sum_{\mathbf{q}'}(t_{\mathbf{q}'} + t_{\mathbf{p}+\mathbf{k}-\mathbf{q}'} - V_{\mathbf{q}-\mathbf{q}'}) \times L_{\mathbf{q}'}(p+k)\Gamma_0(q', p+k-q'|p, k) \quad (19)$$

only with regard to the dependence on quasimomentum $\mathbf{q}$. Here, we use the function $L_{\mathbf{q}}(p+k)$ introduced in [20] that is defined by the expression

$$L_{\mathbf{q}}(p+k) = \frac{n_{\mathbf{q}} + n_{\mathbf{p}+\mathbf{k}-\mathbf{q}} - 1}{i\omega_n + i\omega_m - \varepsilon_{\mathbf{q}} - \varepsilon_{\mathbf{p}+\mathbf{k}-\mathbf{q}} + 2\mu}. \quad (20)$$

In the nearest-neighbor approximation, the solution of the integral equation (19) can be written as

$$\Gamma(q, p+k-q|p, k) = V_{\mathbf{q}-\mathbf{p}} - t_{\mathbf{p}} - t_{\mathbf{k}} + \sum_{\alpha}(2t(1+\cos Q_\alpha) - 2V\cos q_\alpha)C_\alpha(Q|p, k) + \sum_{\alpha}(2t\sin Q_\alpha - 2V\sin q_\alpha)S_\alpha(Q|p, k), \quad (21)$$

where $Q = p + k$ and the unknown functions C_x, C_y, ..., S_x, S_y, ... obey a simple system of algebraic equations ($\alpha, \beta = x, y, ...$):

$$\sum_{\beta}(\delta_{\alpha\beta} - 2t(1+\cos Q_\beta)A_\alpha + 2VB_{\alpha\beta}) \times C_\beta(Q|p, k) - \sum_{\beta}(2t\sin Q_\beta A_\alpha - 2VP_{\alpha\beta}) \times S_\beta(Q|p, k) = 2V \times \sum_{\beta}(B_{\alpha\beta}\cos p_\beta - P_{\alpha\beta}\sin p_\beta) - (t_{\mathbf{p}} + t_{\mathbf{k}})A_\alpha,$$

$$\sum_{\beta}(\delta_{\alpha\beta} - 2t\sin Q_\beta R_\alpha + 2VW_{\alpha\beta})S_\beta(Q|p, k) - \sum_{\beta}(2t(1+\cos Q_\beta)R_\alpha - 2VP_{\beta\alpha}) \times C_\beta(Q|p, k) = 2V \times \sum_{\beta}(P_{\beta\alpha}\cos p_\beta + W_{\alpha\beta}\sin p_\beta) - (t_{\mathbf{p}} + t_{\mathbf{k}})R_\alpha. \quad (22)$$

The following notation is used in these equations:

$$A_\alpha = \frac{1}{N}\sum_{\mathbf{q}}\cos q_\alpha L_{\mathbf{q}}(Q),$$

$$R_\alpha = \frac{1}{N}\sum_{\mathbf{q}}\sin q_\alpha L_{\mathbf{q}}(Q),$$

$$B_{\alpha\beta} = \frac{1}{N}\sum_{\mathbf{q}}\cos q_\alpha \cos q_\beta L_{\mathbf{q}}(Q), \quad (23)$$

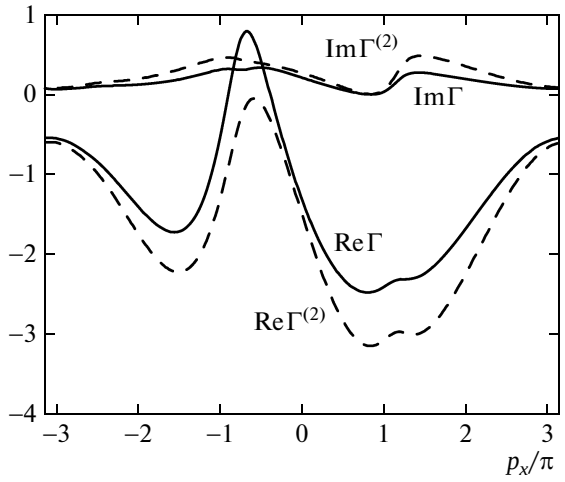

Fig. 7. Real and imaginary parts of the total and Born forward scattering amplitudes.

$$P_{\alpha\beta} = \frac{1}{N}\sum_{\mathbf{q}} \cos q_\alpha \sin q_\beta L_{\mathbf{q}}(Q),$$

$$W_{\alpha\beta} = \frac{1}{N}\sum_{\mathbf{q}} \sin q_\alpha \sin q_\beta L_\beta(Q).$$

A system of four equations arises in the two-dimensional case. The mass operator is known to be expressed in terms of the forward scattering amplitude $\Gamma(p, k|p, k)$. When the total scattering amplitude is used, the intermediate summation over the Matsubara frequencies cannot be performed explicitly, while the application of computer methods requires much time (if it is remembered that the integration should be performed over the quasimomentum $\mathbf{k}$ and, when finding the density of states, also over the quasimomentum $\mathbf{p}$).

We see the way out of this situation in applying a suitable approximation. To justify the approximation used below, we will appeal to an exact solution for the scattering amplitude. A numerical solution of system (22) after substitution into (21) allows the quasimomentum dependence of the ladder forward scattering amplitude $\Gamma(p, k|p, k)$ at various Matsubara frequencies to be compared with the corresponding dependences obtained from an approximate solution for this quantity. Below, the Born approximation will be used as such an approximation. The forward scattering amplitude in the Born approximation will be denoted by $\Gamma^{(2)}(p, k|p, k)$.

Figure 7 shows the dependences on quasimomentum $\mathbf{p}$ in the direction $p_y = p_x$ for the real and imaginary parts of the expressions for Γ and $\Gamma^{(2)}$. In our calculations, we assumed that $V = 1.5$ and $n = 0.8$. The graphical representation for these quantities has the form shown in Fig. 8. As we see, the Born approximation for Γ (without the inhomogeneous part of the integral equation (19)) is obtained by substituting the seed scattering amplitude for the right hatched square (total amplitude). It follows from Fig. 7 that the Born approximation reproduces the features of the quasimomentum dependence of the forward scattering amplitude not only qualitatively but also quantitatively. A similar situation also takes place for other parameters of the system.

Our comparison shows that the Born approximation can be used to take into account the main effects related to the scattering through the kinematic and Coulomb interactions. In this case, the summation over the intermediate Matsubara frequency ω_m in the expression for Σ_B can be performed explicitly. To derive the final formula that includes only the Fermi functions, we applied the technique developed in [21]. As a result, we obtain

$$\Sigma_B(\mathbf{p}, i\omega) = \frac{1}{N^2}\sum_{\mathbf{qk}} \Gamma_0(\mathbf{p}, \mathbf{k}|\mathbf{q}, \mathbf{p}+\mathbf{k}-\mathbf{q}) \times \Gamma_0(\mathbf{q}, \mathbf{p}+\mathbf{k}-\mathbf{q}|\mathbf{p}, \mathbf{k}) + \left\{ \frac{n_{\mathbf{k}}(1-n_{\mathbf{q}}-n_{\mathbf{p}+\mathbf{q}-\mathbf{k}}) + n_{\mathbf{q}} n_{\mathbf{p}+\mathbf{k}-\mathbf{q}}}{i\omega_n + \varepsilon_{\mathbf{k}} - \varepsilon_{\mathbf{q}} - \varepsilon_{\mathbf{p}+\mathbf{q}-\mathbf{k}} + \mu} - \frac{2n_\xi(1-n_\xi)}{i\omega_n - \varepsilon_{\mathbf{q}} + \mu} \right\}, \quad (24)$$

where

$$\Gamma_0(\mathbf{q}, \mathbf{p}+\mathbf{k}-\mathbf{q}|\mathbf{p}, \mathbf{k}) = V_{\mathbf{q}-\mathbf{p}} - t_{\mathbf{p}} - t_{\mathbf{k}},$$

$$n_{\mathbf{q}} = n_{\mathrm{F}}\left(\frac{\varepsilon_{\mathbf{q}}-\mu}{T}\right), \quad n_\xi = n_{\mathrm{F}}\left(\frac{\tilde{\varepsilon}-\mu}{T}\right).$$

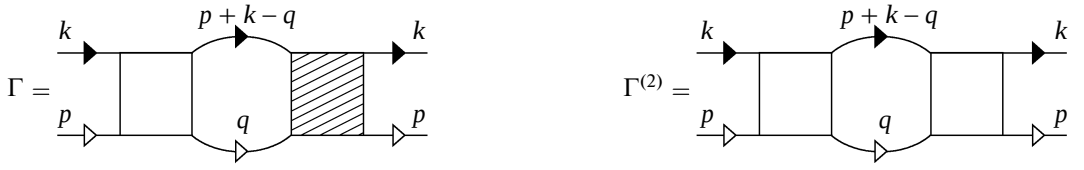

Fig. 8. Graphical representation of the total and Born amplitudes without their homogeneous parts.

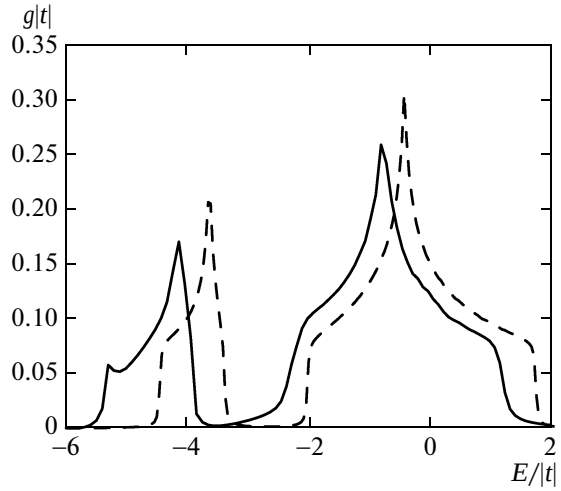

Fig. 9. Densities of states calculated based on the complete mass operator (solid line) and the mass operator in the single-oval approximation (dashed line).

Thus, the complete mass operator is the sum of two terms:

$$\Sigma(\mathbf{p}, i\omega_n) = \Sigma_{\text{oval}}(i\omega_n) + \Sigma_B(\mathbf{p}, i\omega_n). \quad (25)$$

Using the derived expression for the mass operator, it is easy to calculate the density of states after the analytic continuation. Figure 9 shows the results of our numerical calculation for the total density of states (solid line) at the same parameters as those in Fig. 7. To clarify the relative contribution $\Sigma_B(\mathbf{p}, i\omega_n)$, the dashed line in the same figure for the same set of parameters indicates the density of states obtained in the single-oval approximation, i.e., when $\Sigma(\mathbf{p}, i\omega_n) = \Sigma_{\text{oval}}(i\omega_n)$. Comparison of the presented dependences shows that (1) going outside the scope of the single-oval approximation leads to a slight shift in energy of the density of states; the upper band undergoes changes near the top; (2) the lower band (BFS) is broadened; and (3) the emergence of an imaginary part of the mass operator leads to a partial blurring of the gap between BFS and the main band. At the same time, it should be emphasized that the main peculiarity related to the formation of a split-off BFS is retained and is described mainly by the mass operator obtained in the single-oval approximation.

6. THE INFLUENCE OF THE BAND OF FLUCTUATION STATES ON THE CONCENTRATION DEPENDENCE OF THE SUPERCONDUCTING PHASE TRANSITION TEMPERATURE

In Section 4, the induction of BFS was shown to lead to a redistribution of the spectral intensity of the electron correlation function. This effect grows with increasing doping level and, hence, can affect the concentration dependence of the critical superconducting transition temperature. We will investigate this question based on the method developed in [7].

The behavior of the critical superconducting transition temperature with changing model parameters (e.g., the electron concentration) can be studied by analyzing the pole of the scattering amplitude in the Cooper channel. In graphical form, this amplitude $\Gamma(p, -p|k, -k) \equiv \Delta(p|k)$ obeys the ladder equation displayed in Fig. 10, where the light square corresponds to the seed scattering amplitude $\Gamma_0(p, -p|k, -k) \equiv \Delta_0(p|k)$. Here, we assume that $p \equiv (\mathbf{p}, i\omega_n)$ and $k \equiv (\mathbf{k}, i\omega_m)$.

The specific form of the solution of the integral equation for $\Delta(p|k)$ depends both on the structure of the seed amplitude $\Delta_0(p|k)$ (i.e., the pattern of the dependences on quasimomenta and Matsubara frequencies) and on the Green functions $G(\mathbf{q}, i\omega_l)$ and $G(-\mathbf{q}, -i\omega_l)$ appearing in this equation. In the case where these functions were taken without allowance for the effects attributable to the formation of BFS, the solutions for the homogeneous part of the integral equation for the scattering amplitude were studied in detail in [7].

Describing the effects attributable to the induction of BFS is formally reduced to using the function

$$G(\mathbf{q}, i\omega_n) = \frac{i\omega_n - \zeta + \mu}{(i\omega_n - E_{\mathbf{q}}^{+} + \mu)(i\omega_n - E_{\mathbf{q}}^{-} + \mu)}, \quad (26)$$

derived from Eq. (11), given that $D(\mathbf{q}, i\omega_l) = (1 - n/2)G(\mathbf{q}, i\omega_l)$ in the approximation under consideration, as the Green function.

Let us analyze the changes in the concentration dependence of the critical temperature related to the formation of BFS with increasing doping level. For clarity, we will restrict ourselves to solving the problem without allowance for the scattering by spin fluctua-

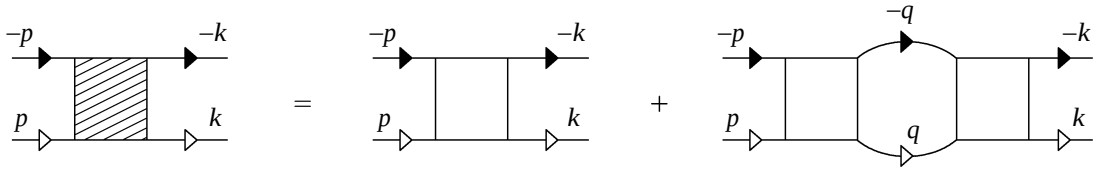

Fig. 10. Equation for the Cooper scattering amplitude.

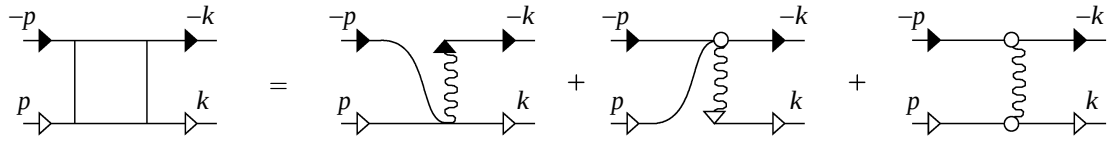

Fig. 11. Graphical representation for the seed Cooper vertex.

tions. In this case, the seed amplitude reflects well the known processes [7] and has the graphical representation shown in Fig. 11. Analytically, this amplitude is defined by the expression

$$\Delta_0(p|k) = V_{\mathbf{p}-\mathbf{k}} - 2t_{\mathbf{k}}. \tag{27}$$

Once the analytical expressions have been brought into correspondence to the diagrams of Fig. 10 and allowance has been made for the fact that the seed scattering amplitude is independent of the Matsubara frequency, we obtain an integral equation for $\Delta(\mathbf{p}|\mathbf{k})$,

$$\Delta(\mathbf{p}|\mathbf{k}) = V_{\mathbf{p}-\mathbf{k}} - 2t_{\mathbf{k}} - \frac{1}{N}\sum_{\mathbf{q}}(V_{\mathbf{p}-\mathbf{q}} - 2t_{\mathbf{q}})\tilde{L}(\mathbf{q})\Delta(\mathbf{q}|\mathbf{k}), \tag{28}$$

where, as in [20],

$$\tilde{L}(\mathbf{q}) = T\sum_{\omega_l} G(\mathbf{q}, i\omega_l)G(-\mathbf{q}, -i\omega_l). \tag{29}$$

Summing over the Matsubara frequencies yields function (29) in explicit form:

$$\tilde{L}(\mathbf{q}, T_c) = \frac{(E_{\mathbf{q}}^{+} - \zeta)(E_{\mathbf{q}}^{+} + \zeta - 2\mu)}{4\nu_{\mathbf{q}}(E_{\mathbf{q}}^{+} + E_{\mathbf{q}}^{-} - 2\mu)(E_{\mathbf{q}}^{+} - \mu)}\tanh\left(\frac{E_{\mathbf{q}}^{+} - \mu}{2T_c}\right) - \frac{(E_{\mathbf{q}}^{-} - \zeta)(E_{\mathbf{q}}^{-} + \zeta - 2\mu)}{4\nu_{\mathbf{q}}(E_{\mathbf{q}}^{+} + E_{\mathbf{q}}^{-} - 2\mu)(E_{\mathbf{q}}^{-} - \mu)}\tanh\left(\frac{E_{\mathbf{q}}^{-} - \mu}{2T_c}\right). \tag{30}$$

We see that allowance for BFS leads to a modification of the homogeneous part of the integral equation that consists in the replacement of the function

$$L(\mathbf{q}) = \frac{1}{2(\varepsilon_{\mathbf{q}} - \mu)}\tanh\left(\frac{\varepsilon_{\mathbf{q}} - \mu}{2T}\right) \tag{31}$$

by the function $\tilde{L}(\mathbf{q})$.

Applying the technique for solving Eq. (28) described in [7], we find that the amplitude $\Delta(\mathbf{p}|\mathbf{k})$ for the class of solutions under consideration is expressed in terms of two unknown functions (d is the system's dimension):

$$X_{\mathbf{k}} = \frac{1}{N}\sum_{\mathbf{q}}\left(\sum_{i=1}^{d}\cos q_i\right)\tilde{L}(\mathbf{q})\Delta(\mathbf{q}|\mathbf{k}),$$
$$Y_{\mathbf{k}} = \frac{1}{N}\sum_{\mathbf{q}} R_{\mathbf{q}}\tilde{L}(\mathbf{q})\Delta(\mathbf{q}|\mathbf{k}) \tag{32}$$

via the equation

$$\Delta(\mathbf{p}|\mathbf{k}) = V_{\mathbf{p}-\mathbf{k}} - 2t_{\mathbf{k}} + \left(4t - \frac{V_{\mathbf{p}}}{d}\right)X_{\mathbf{k}} + 2Y_{\mathbf{k}}. \tag{33}$$

To calculate these functions, we can obtain the system of two algebraic equations

$$\left(1 - 4tA_1 + \frac{2V}{d}A_2\right)X_{\mathbf{k}} - 2A_1 Y_{\mathbf{k}} = \frac{V_{\mathbf{k}}}{d}A_2 - 2t_k A_1,$$
$$(VB_R - 4tA_R)X_{\mathbf{k}} + (1 - 2A_R)Y_{\mathbf{k}} = \frac{V_{\mathbf{k}}}{d}B_R - 2t_{\mathbf{k}}A_R. \tag{34}$$

The following notation is used in system (34):

$$A_1(T) = \frac{1}{N}\sum_{\mathbf{q}}\left(\sum_{i=1}^{d}\cos q_i\right)\tilde{L}(\mathbf{q}),$$
$$A_2(T) = \frac{1}{N}\sum_{\mathbf{q}}\left(\sum_{i=1}^{d}\cos q_i\right)^2\tilde{L}(\mathbf{q}),$$
$$A_R(T) = \frac{1}{N}\sum_{\mathbf{q}} R_{\mathbf{q}}\tilde{L}(\mathbf{q}),$$
$$B_R(T) = \frac{2}{dN}\sum_{\mathbf{q}}\left(\sum_{i=1}^{d}\cos q_i\right)R_{\mathbf{q}}\tilde{L}(\mathbf{q}). \tag{35}$$

The quantities $A_R(T)$ and $B_R(T)$ appear, because the hoppings into far coordination spheres are taken into account. In this case, the complete Fourier transform of the hopping integral $t_{\mathbf{k}}$ has form (17).

From the condition for the determinant of system (34) being equal to zero, we derive an equation for the critical temperature:

$$1 + \frac{2V}{d}A_2(T_c) + 2VA_1(T_c)B_R(T_c) = 4tA_1(T_c) + 2A_R(T_c)\left(1 + \frac{2V}{d}A_2(T_c)\right). \tag{36}$$

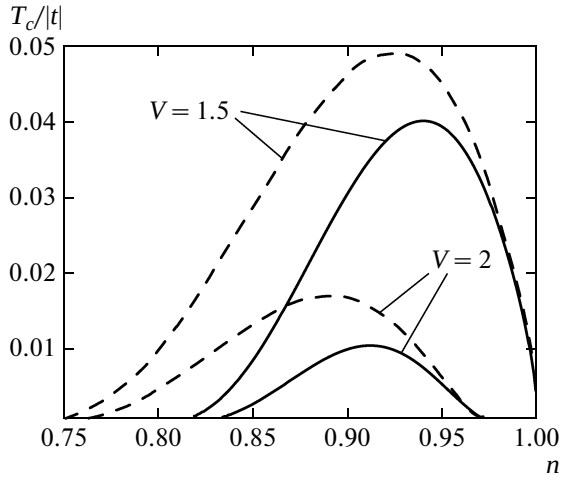

Fig. 12. Superconducting transition temperature versus electron concentration.

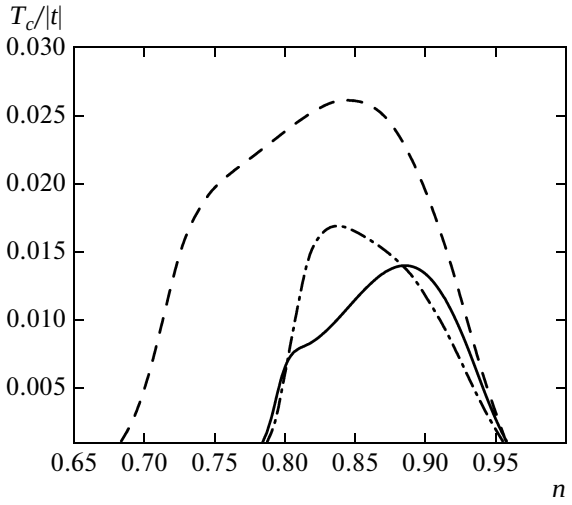

Fig. 13. Modification of the concentration dependence of the critical superconducting phase transition temperature with allowance made for long-range hoppings ($V = 2$).

In the nearest-neighbor approximation, $A_R = B_R = 0$ and, as a result, we obtain a simpler equation,

$$1 + V\frac{1}{N}\sum_{\mathbf{q}}(\cos q_x + \cos q_y)^2\tilde{L}(\mathbf{q}) = 4t\frac{1}{N}\sum_{\mathbf{q}}(\cos q_x + \cos q_y)\tilde{L}(\mathbf{q}). \quad (37)$$

Without allowance for BFS, the equality $\tilde{L}(\mathbf{q}) = L(\mathbf{q})$ holds. In this limiting case, Eq. (37) completely corresponds to Eq. (23) from [7].

The results of our numerical calculations to determine the concentration dependences of the chemical potential and critical temperature T_c are presented in Fig. 12. The solid lines indicate the dependences $T_c(n)$ obtained by solving Eq. (37). For comparison, the dashed lines in the same figure indicate the dependences $T_c(n)$ obtained by solving the same equation but at $\tilde{L}(\mathbf{q}) = L(\mathbf{q})$, i.e., when the effect of BFS induction is disregarded. We see that in the range of electron concentrations n close to unity, the influence of BFS is insignificant (the solid and dashed lines coincide). This is natural, because the spectral intensity of BFS becomes zero when $n \longrightarrow 1$. If the concentration increases, then the rms fluctuation of the occupation numbers also grows. In this case, the spectral intensity for BFS becomes high and the contribution of BFS is great. We see from the figure that in the most interesting range of electron concentrations $n \approx 0.8$–0.9, the renormalization of the critical temperature is comparable to or even exceeds the value of T_c itself calculated without allowance for the contributions from BFS. Thus, the effects related to the induction of BFS affect significantly the phase diagram of the system in the range of concentrations where the superconducting state takes place.

When the hoppings into far coordination spheres are taken into account, the critical temperature can be determined from the solution of Eq. (36). The presence of such hoppings leads to a change in the shape of the curve $T_c(n)$. The combined effect of the far hoppings and BFS on the dependence $T_c(n)$ is demonstrated in Fig. 13. The dashed line represents the dependence $T_c(n)$ calculated without allowance for BFS for the set of parameters $t' = -0.1$, $t'' = 0.05$, and $V = 2$. It follows from our comparison with the dashed curve in Fig. 12 calculated for $V = 2$ that allowance for the long-range hopping deforms significantly the dependence $T_c(n)$ in the range of low electron concentrations. Allowance for BFS (solid line) leads to a nonuniform suppression of the critical temperature and a further deformation of the curve $T_c(n)$. An increase in the hopping parameter t'' when BFS is taken into account leads to a shift in the peak of the curve $T_c(n)$ toward lower electron concentrations ($t'' = 0.1$, the dash–dotted line).

Summing up this part of our study, it should be noted that the influence of the intersite Coulomb interaction manifests itself in two ways. First of all, as was shown in [7], the intersite Coulomb interaction causes a strong suppression of the superconducting phase region. The second effect related to the fluctuation of the setting single-ion one-electron energy when the intersite interaction is taken into account leads to a nonuniform (in concentration) decrease in critical temperature. It is this nonuniform renormalization that constitutes the main content of the effect attributable to allowance for BFS in the Shubin–Vonsowsky model.

7. CONCLUSIONS

The presented results of our study of the influence of strong intersite correlations on the energy structure and spectral characteristics of narrow-gap Mott–Hubbard insulators at a low doping level show the existence of two qualitatively new effects.

The first effect is related to the formation of a new energy band mediated by charge fluctuations. As has already been noted above, these fluctuations lead to a change in the effective one-site energy. Therefore, under conditions of a relatively weak hopping integral (narrow gap), this change is comparable to or exceeds the gap width. It is these factors that underlie the physical nature of the formation of a split-off band of fluctuation states. It should be specially emphasized that the effect being discussed is attributable precisely to correlation contributions and not just to a strong intersite interaction. Indeed, since the interaction under consideration is a two-site one, its significant contribution is reduced to mean-field renormalizations that do not lead to the induction of a band of fluctuation states. In this case, the appearance of an additional band was initiated by the two-pole structure of the one-electron Green function obtained after the substitution of the mass operator. This operator was calculated when allowance was made for an infinite sequence of diagrams that reflect the main contributions from intersite correlations.

The second effect is related to a redistribution of the spectral intensity between the main zone and the zone of fluctuation states. Without doping, the spectral intensity of the additional zone is zero. The physical cause of this effect is that the configuration environment of each ion corresponds to the nominal one. Mathematically, this is reflected by a zero rms fluctuation of the occupation numbers. As the doping level increases, the spectral intensity of the main band decreases, while the spectral intensity of the fluctuation band increases. As a result of this effect, a nonuniform (in electron concentration) renormalization of the superconducting transition temperature noted in the preceding section takes place.

Another manifestation of the spectral intensity redistribution is related to a drop in the density of states at the Fermi level and an increase in the number of points of the Brillouin zone under the Fermi surface (or contour). This effect will affect significantly the quantum phase transitions related to a change in the topology of the Fermi contour in the case of doping [22]. It follows from the modification of the density of electronic states and the chemical potential shift that intersite correlations can also initiate a decrease in the Sommerfeld coefficient in the electronic part of the specific heat and renormalize the frequency of magnetic susceptibility oscillations in the de Haas–van Alphen effect.

ACKNOWLEDGMENTS

We express our deep gratitude to R.O. Zaitsev for numerous remarks and discussions. We are grateful to A.A. Golovnya, A.A. Shklyaev, and V.A. Mitskan for specific advice on the numerical calculations of the mass operator. This work was supported by the "Quantum Condensed Matter Physics" Program of the Presidium of the Russian Academy of Sciences, the Russian Foundation for Basic Research (project no. 10-02-00251), the "Scientific and Scientific–Pedagogical Personnel of Innovational Russian for 2009–2013" Federal Goal-Oriented Program, and the Interdisciplinary Integration Project no. 53 of the Siberian Branch of the Russian Academy of Sciences. One of us (M.K.) thanks Lavrentiev's contest of youth projects of the Siberian Branch of the Russian Academy of Sciences.

REFERENCES

1. N. F. Mott, *Metal–Insulator Transitions* (Taylor and Francis, London 1974; Nauka, Moscow, 1979).
2. J. C. Hubbard, Proc. R. Soc. London, Ser. A **276**, 238 (1963).
3. J. C. Hubbard, Proc. R. Soc. London, Ser. A **285**, 542 (1965).
4. R. O. Zaitsev, Zh. Eksp. Teor. Fiz. **68** (1), 207 (1975) [Sov. Phys. JETP **41** (1), 100 (1975)]; Zh. Eksp. Teor. Fiz. **70** (3), 1100 (1976) [Sov. Phys. JETP **43** (3), 574 (1976)].
5. R. O. Zaitsev, Zh. Eksp. Teor. Fiz. **78** (3), 1132 (1980) [Sov. Phys. JETP **51** (3), 571 (1980)].
6. R. O. Zaitsev, Preprint IAE-3927/1 (I. V. Kurchatov Institute of Atomic Energy, Moscow, 1984).
7. R. O. Zaitsev, Zh. Eksp. Teor. Fiz. **125** (4), 891 (2004) [JETP **98** (4), 780 (2004)].
8. S. Shubin and S. Vonsowsky, Proc. R. Soc. London, Ser. A **145**, 159 (1934).
9. S. Shubin and S. Vonsowsky, Phys. Z. Sowjetunion **7**, 292 (1935); Phys. Z. Sowjetunion **10**, 348 (1936).
10. R. O. Zaitsev, V. A. Ivanov, and Yu. V. Mikhailova, Fiz. Met. Metalloved. **65**, 1032 (1988); Fiz. Met. Metalloved. **68**, 1108 (1989).
11. V. I. Belyavskii and Yu. V. Kopaev, Usp. Fiz. Nauk **176** (5), 457 (2006) [Phys.—Usp. **49** (5), 441 (2006)].
12. A. A. Ovchinnikov, M. Ya. Ovchinnikova, and E. A. Plekhanov, Zh. Eksp. Teor. Fiz. **115** (2), 649 (1999) [JETP **88** (2), 356 (1999)].
13. A. A. Ovchinnikov and M. Ya. Ovchinnikova, Zh. Eksp. Teor. Fiz. **118** (6), 1434 (2000) [JETP **91** (6), 1242 (2000)].
14. L. M. Falicov and J. C. Kimball, Phys. Rev. Lett. **22**, 997 (1969).
15. D. I. Khomskii, Usp. Fiz. Nauk **129** (2), 443 (1979) [Sov. Phys.—Usp. **22** (10), 879 (1979)].

16. R. O. Zaitsev, *Diagram Methods in the Theory of Superconductivity and Magnetism* (Editorial URSS, Moscow, 2004) [in Russian].
17. Yu. A. Izyumov and B. M. Letfulov, J. Phys.: Condens. Matter **2**, 8905 (1990).
18. V. G. Bar'yakhtar, V. E. Krivoruchko, and D. A. Yablonskii, *Green's Functions in the Theory of Magnetism* (Naukova Dumka, Kiev, 1984) [in Russian].
19. V. V. Val'kov and S. G. Ovchinnikov, *Quasiparticles in Strongly Correlated Systems* (Siberian Branch of the Russian Academy of Sciences, Novosibirsk, 2001) [in Russian]; S. G. Ovchinnikov and V. V. Val'kov, *Hubbard Operators in the Theory of Strongly Correlated Electrons* (Imperial College Press, London, 2004).
20. R. O. Zaitsev, Pis'ma Zh. Eksp. Teor. Fiz. **86** (1), 54 (2007) [JETP Lett. **86** (1), 51 (2007)].
21. V. M. Galitskii, Zh. Eksp. Teor. Fiz. **34** (1), 151 (1958) [Sov. Phys. JETP **7**, (1), 104 (1958)].
22. S. G. Ovchinnikov, M. M. Korshunov, and E. I. Shneyder, Zh. Eksp. Teor. Fiz. **136** (5), 898 (2009) [JETP **109** (5), 775 (2009)].

Translated by V. Astakhov